X-ray Spectromicroscopy of Polymers:
An introduction for the non-specialist[++]

Ivaylo Koprinarov and Adam P. Hitchcock
BIMR, McMaster University
Hamilton, ON Canada L8S 4M1

1. Introduction

X-ray absorption spectroscopy has advanced rapidly in the last decades, particularly with synchrotron radiation based techniques [stohr 92]. The high brightness of the synchrotron X-ray source has allowed tremendous improvements in spectral resolution and the development of X-ray microscopies which apply X-ray absorption spectroscopy to heterogeneous materials at high spatial resolution. Novel characterisation techniques are being developed [ade 98] which allow both *spectromicroscopy* - imaging with spectral sensitivity, and *microspectroscopy* - recording spectra from very small spots. We choose to call these novel analytical tools *X-ray spectromicroscopy*, to emphasize that it is the combination of spectroscopy and microscopy that is the essence of these techniques. This article describes one of these techniques, *scanning transmission x-ray microscopy* (STXM) [ade 97, warwick 97, warwick 98], and illustrates its capabilities through two selected applications in polymer analysis [ade 92, ade 93, ade 95, smith 96]. Authoritative reviews of STXM have been published which stress materials [ade 98, ade00] and biological [kirz 95] applications.

There are many problems in polymer physics and chemistry which require detailed chemical analysis at a sub-micron spatial scale - phase segregation; determination of the morphology and interface chemistry of blends and co-polymer systems; nano-patterned structures, self assembly; and many others. 'Traditional' chemical spectroscopies used for polymer studies such as infrared and nuclear magnetic resonance can differentiate chemical species but they do not have the necessary sub-micron spatial resolution. Analytical transmission and scanning transmission electron microscopy have excellent spatial resolution and are very useful to visualise the structure, but electron microscopy typically does not have sufficient chemical sensitivity for

---

[+] This document is posted on the web site of the Hitchcock group (unicorn.mcmaster.ca). It is intended to be an informal introduction of a tutorial nature, rather than an historical or comprehensive overview. Please see the articles referenced for more complete presentations of the technique and its many applications.

quantitative chemical mapping beyond the elemental level. In many cases it is ambiguous whether structure observed by electron (or optical) microscopy arises from chemical differences or if it is simply caused by density/thickness variations or reflectivity changes (optical). In addition, electron microscopy of polymers is experimentally difficult on account of high rates of radiation damage by energetic electron beams [Egerton 87].

Fig. 1 X-ray absorption edges of carbon, nitrogen and oxygen of a composition typical of a polymer. A rapid increase of the absorption occurs at the threshold of energy required to excite electrons from these inner shells.

2. Near Edge X-ray Absorption Fine Structure

As an x-ray passes through matter, it is absorbed to an extent which depends on the nature of the substance, the thickness of the sample, and the density of the sample. The absorbed photons cause excitation of the inner shell electrons of the atoms in the substance. These excited inner shell (core) electrons can be promoted to unoccupied energy levels to form a short lived *excited state* or they can be removed completely to form an *ionized state*. Traditionally, X-ray absorption spectroscopy was described in terms of *absorption edges* which are the onsets of inner-shell ionization (**Figure 1**). There is an absorption edge associated with each inner shell energy level of an atom, such that all elements have an X-ray absorption edge in the soft X-ray energy range (100-1200 eV). The amount of a particular element can be determined quantitatively from the difference in the x-ray absorption just above and just below its absorption edge.

While this traditional aspect of X-ray absorption provides the basis for elemental analysis, the modern technique as practised at synchrotron facilities is much more powerful. It can identify and quantitate the chemical structure of the element from the fine scale details of the absorption spectrum that occur at each edge, the so-called *near-edge x-ray absorption fine structure* or NEXAFS [Stohr 92].
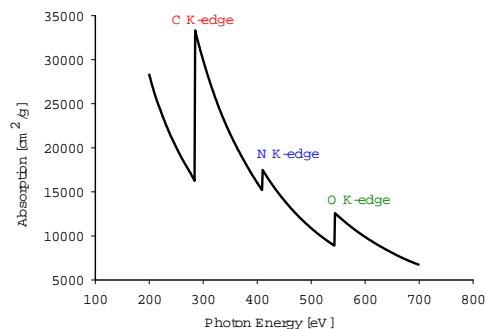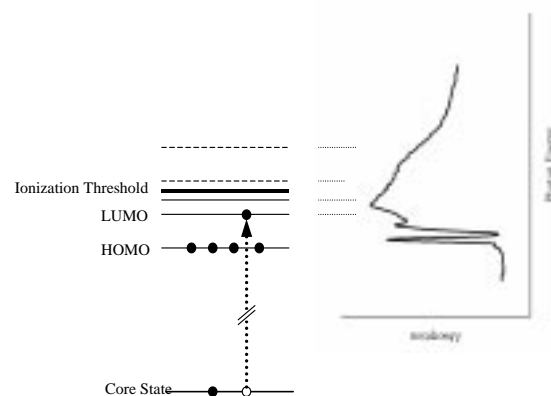

Fig. 2 The near edge x-ray absorption fine structure (NEXAFS) arises from electronic transitions of an inner shell electron to energy levels (orbitals in molecules, bands in solids) which are normally unoccupied in the ground state. The lowest unoccupied molecular orbital (LUMO) is the π* orbital in essentially all unsaturated compounds.
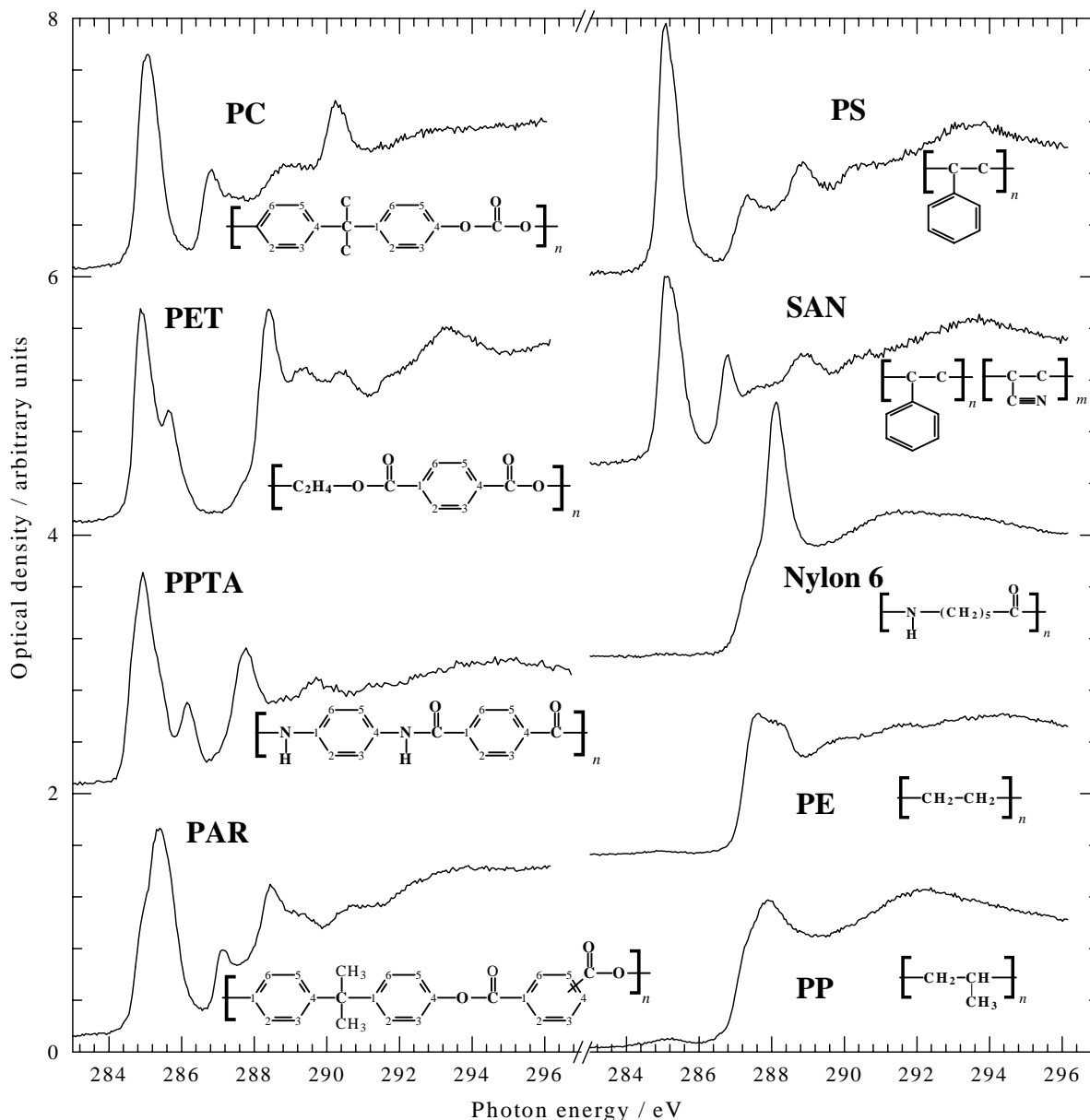
Fig. 3 C 1s NEXAFS spectra of some common polymers. Abbreviation as follows: PC, polycarbonate; PET, poly(ethylene terephthalate); PPTA, poly(p-phenylene terephthalamide); PAR, polyacrylate; PS, polystyrene; SAN, styrene-acrylonitrile; Nylon-6, poly(ε-caprolactam); PP, polypropylene; PE, polyethylene. (Figure adopted from [Ade 97])

These features, which can be as much as 10 times stronger than the absorption edge jump, correspond to electronic excited states in which an inner-shell electron has been excited to unfilled molecular orbitals or conduction bands. As the x-ray energy is increased throughout an absorption edge, first there is structure associated with excitation to the lowest unoccupied molecular orbital, which is a π^* orbital for unsaturated molecules (double or triple bonds), followed by structures associated with higher energy unoccupied molecular orbitals, typically of σ^* character associated

with saturated (single) chemical bonds, and then direct inner-shell ionization (**Figure 2**). The unoccupied electronic structure and thus the inner-shell excited states are determined by the geometric and electronic (bonding) structure of the sample. NEXAFS spectra differ significantly even for rather similar molecular structures, as shown in **Figure 3** for some common polymers [Ade 97b]. This means that the NEXAFS spectrum of each polymer can be used as a *fingerprint*. In many cases, enough is known about how chemical structure and X-ray absorption spectral features are related to allow one to identify unknown species from measured NEXAFS spectra. Individual spectral features, particularly the low energy π^* features, are often sufficient for qualitative identification in reasonably well characterized systems, and they can serve as useful energies for selective chemical contrast in X-ray microscopy. There is characteristic NEXAFS structure at the absorption edge of each element in a sample. Thus combined studies of C 1s, N 1s and O 1s NEXAFS is a very powerful tool in polymer analysis. Finally, comparisons with NEXAFS spectra of pure standards provides a means to derive *quantitative composition maps* of the components of a complex material from a series of X-ray microscopy images.

3. Scanning Transmission X-ray Microscope (STXM): Simple Description and Operation

A simplified view of STXM is shown in **Figure 4**. A *Fresnel zone plate* focuses mono-energetic X-rays provided by a suitable *monochromator* beamline mounted on a suitable, bright synchrotron source. The focal point is typically 50 nm in diameter over a 3-10 μm waist. An image is generated by monitoring the X-ray signal transmitted through a thin section of a specimen as it is raster-scanned at the focus of the x-rays. Micro-spectra are measured by holding the beam at the spot of interest on the sample while the photon

Fig. 4 Schematic scanning x-ray transmission microscope (STXM). A Fresnel zone plate is used to focus the x-rays in the sample plane. To generate an image, a thin section of a specimen is raster-scanned in the focus of the x-rays under computer control. The transmitted photons are counted behind the sample by an x-ray sensitive detector.

energy is scanned. The sample in a STXM can be mounted in air (with sufficiently short X-ray path length), in He at atmospheric pressure, or even sandwiched between two X-ray transparent silicon nitride windows. The latter approach is used to study wet samples such as hydrated polymers [Mitchell99] or biological material [Kirz95].
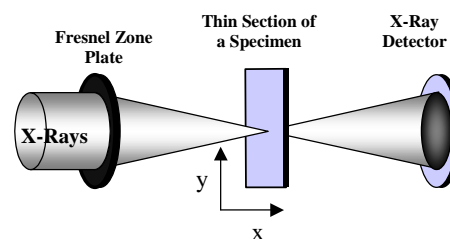
The STXM at the *Advanced Light Source* (ALS) which we use can record images with better than 100 nm spatial resolution, and NEXAFS spectra from 150 - 1400 eV with an energy resolution of about 100 meV [warwick 97, warwick 98]. Samples must be partly transparent at the X-ray energy of interest, which means a sample thickness of 50 to 300 nm for carbon studies, ranging up to 1 - 2 microns thick for higher energy edges or low density samples such as hydrated polymer gels or biological samples. The sample preparation challenges are similar to those encountered for analytical transmission electron microscopy. Microtomed sections about 100 nm thick which are mounted on 3 mm metal grids are a common form of sample. We use silicon wafers with X-ray transparent, 100 nm thick silicon nitride windows (of up to 4 mm lateral size) to study samples in water. One can even do N 1s spectroscopy through these windows. A strength of STXM relative to electron microscopy is that radiation damage is two orders of magnitude less than in electron beam imaging techniques [rightor 97], making this technique ideally suited for radiation sensitive polymers.

The transmitted X-ray signal is measured by single photon counting using counting periods (dwell times) of 0.2 - 0.5 ms per pixel for imaging. A 300x300 pixel image takes about 30 seconds to acquire. Typically, many problems can be solved by measuring a small number of images at selected, chemically sensitive images. In cases where one needs a very detailed chemical analysis of a specific region it is useful to take a systematic series of images at a fine mesh of energies around the absorption edge of interest. These *image sequences* - which might involve one hundred 100x200 pixel images, or about 8 Mb of raw data - can be processed off-line in a variety of ways for both qualitative species identification and to derive quantitative composition maps. Examples of these approaches are shown below.

For quantitative analysis, the transmitted signal is converted to an optical density (OD) according to

$$OD = ln(I_o/I)$$

where for a given X-ray energy I_0 is the incident x-ray flux, I is the transmitted flux through the sample, and ln is the natural logarithm. The OD is related to the sample properties by

$$OD = \mu(E).\rho.t$$

where $\mu(E)$ is the mass absorption coefficient at X-ray energy E, ρ is the density and t is the sample thickness. The mass absorption coefficient is derived from measurements of the NEXAFS spectra of the pure material. Practically, spectra are obtained by first recording an energy scan I

from the spot of interest and subsequently the incident flux I_o measured with the same detector and optical path but with the sample out of the beam. Typically, this takes a few minutes.

4. Example 1: Qualitative polymer analysis

This is part of a study [Hitchcock 00] of reinforcing filler particles which are used in moulded compressed polyurethane foams in the automotive and furnishing industries to achieve higher hardness and load bearing capability. STXM was been used to study two types of copolymer polyol (CPP) fillers – hard polymer particles dispersed in a polyether polyol - present in a toluene di-isocyanate-based polyurethane. One CPP is a copolymer styrene and acrylonitrile (SAN). The other CPP is an aromatic-carbamate

Fig. 5 Transmission electron microscope image of a polyurethane section containing a mixture of two types of copolymer polyol particles: SAN - a copolymer of polystyrene and polyacrylonitrile, and PIPA - a carbamate-rich polyisocyanate polyaddition product.

rich **p**oly-**i**socyanate **p**oly-**a**ddition product (PIPA), derived from methylene diisocyanate. Both particles are chemically indistinguishable by transmission electron microscopy (**Figure 5**) although the size and spatial distribution are clearly revealed.
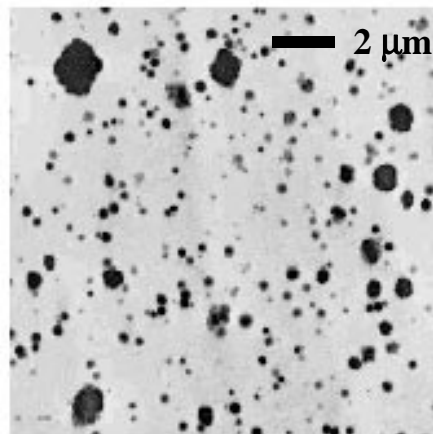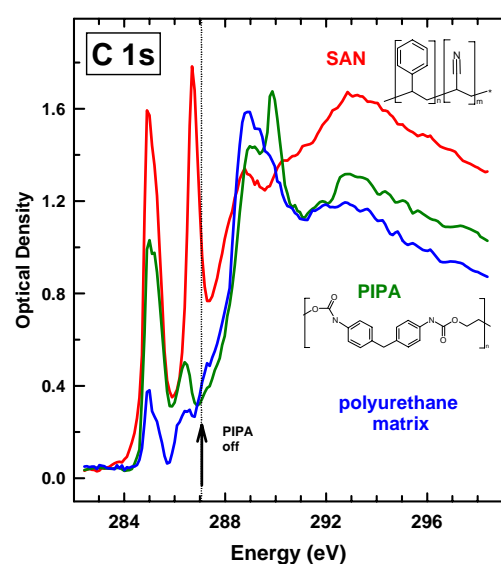

Fig. 6 C 1s NEXAFS spectra in optical density (OD) of the polyurethane matrix, PIPA particles and SAN particles.

Chemical selective imaging in the C 1s NEXAFS (**Figure 6**) identifies the SAN and PIPA particles unambiguously. Since the spectra of both SAN and PIPA absorb strongly at 285.0 eV associated with the phenyl groups of the aromatic filler particles, images at 285.0 eV show both types of particles and thus the 285 eV image (**Figure 7a**) is identical to the electron microscopy image. Only SAN has a strong absorption at 286.7 eV, associated with the acrylonitrile component (AN). Thus imaging at 287 eV, on the higher energy side of this peak where the optical density of the PIPA particles and the matrix is the same and low compared to the SAN particles,
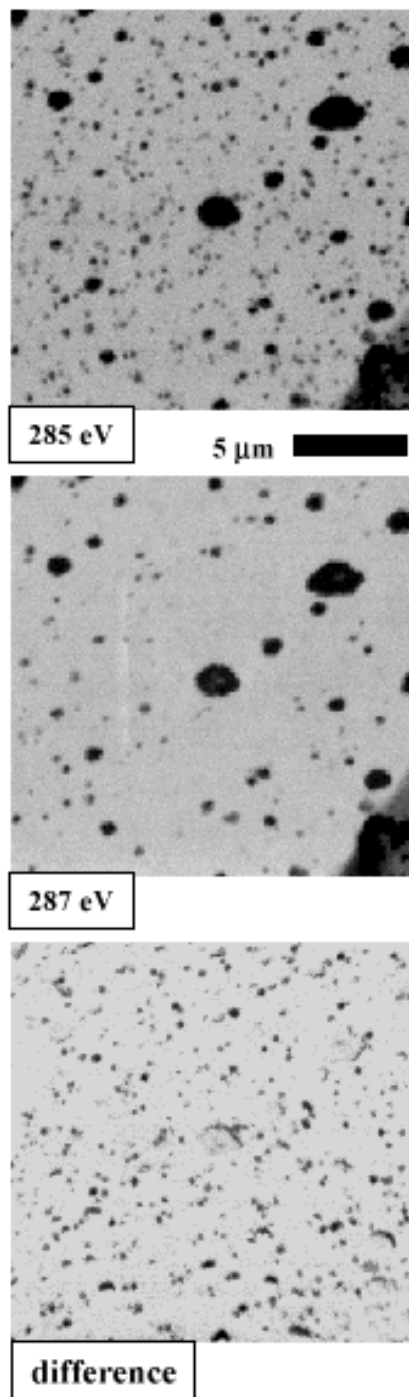
Fig. 7 Comparison of images at 285 eV and 287 eV of the polyurethane with SAN and PIPA filler particles. The third image is the difference of the 285 and 287 eV images, which highlights the PIPA particles only.

gives an image in which only SAN particles are in high contrast (**Figure 7b**). After subtracting the 287 eV from the 285 eV image, the PIPA particles can be identified without difficulty (**Figure 7c**). This example dramatically demonstrates that NEXAFS microscopy can be a quick and reliable means to differentiate chemical species at a sub-micron spatial scale. Further analysis of this material has lead to full quantification of the CPP particle compositions, and detailed size distribution analyses for each type of particle. Neither of these aspects would have been achievable by analytical electron microscopy.

5. Image processing and advanced results

Recording sequences of images with short dwell time and fine energy spacing can be very useful [jacobsen 00]. For instance, post-processing of the images series can be used to extract spectra at any subset of pixels in the sampled region, long after the measurement is finished. This approach can provide serendipitous discoveries. An example of this for the PIPA-SAN polyurethane filler particle system is shown in **Figure 8**. Relative to multiple single point measurements, image sequence procedures also minimize radiation damage. At the ASL point spectra cannot be acquired without exposing the sample to ~200 msec per energy point, or say, 20 seconds for a 100 point energy scan. In contrast, image sequences which can provide statistical precision of 1-2% in a 0.2x0.2 μm region can be acquired with dwell times per pixel of 0.5 msec, or 50 msec total for the full 100-point energy spectrum. Of course damage is not restricted solely to the point sampled but even so, there is a reduction in dose of several orders of magnitude relative to
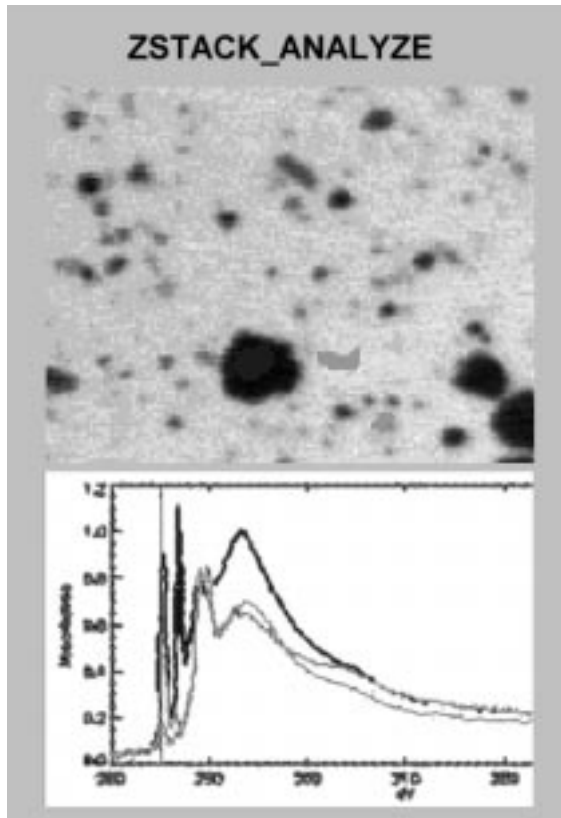
Fig. 8 Example of extracting spectra from different regions of an image sequence (stack). Software is AXIS2000, using stack analysis routines developed by *Chris Jacobsen* (Physics, SUNY-Stony Brook) and *Carl Zimba* (Photons Unlimited) [jacobsen 00].

point scan mode.

Another application of image sequences is *quantitative analysis*. The absorption signal from a given column of the sample is related to the amount of each component, the x-ray absorption response of each component, and the overall thickness and density of the material in the column. Since NEXAFS spectra for pure materials can be obtained with accurate mass absorption scales, STXM can be used for quantitative analysis at sub-micron ranges [Koprinarov 00]. Quantitative composition maps can be derived by two different approaches *singular value decomposition* (SVD) [Koprinarov 00] and *image sequence fits* [Kneedler 00]. A brief description of each follows.

Singular value decomposition

The optical density is determined by the formula $OD = \mu.\rho.t$, where μ is the energy-dependent mass absorption coefficient (cm^2/g), ρ is the density (g/cm^3), and t is the sample thickness (cm). If the mass absorption coefficients of each components are known at the energies sampled, the problem can be converted to a simple superposition and linear algebra can be used to convert sets of images into equivalent thickness ($\rho t(x,y)$) or composition maps. In principle, the decomposition problem can be expressed as a matrix equation $A\boldsymbol{x}=\boldsymbol{d}$, where x is a vector describing the unknown distribution of each component (ρt), $\boldsymbol{d}$ are the measured images (converted to OD scale), and A is the matrix of the mass absorption coefficients (μ) obtained from reference spectra for each component, converted to mass absorption scale. The advantage of the singular value decomposition procedure is that, once the absorption coefficients for a set of materials and energies are known, one can calculate *a priori* the matrix which will optimally invert an over-

determined sampling of energies into the best possible component maps. It can be shown that the SVD solution is the least squares solution [strang 88, press 92].

Image sequence fits

Image sequence fitting [hitchcock 00] computes a least squares fit of the intensity at each pixel(j,k) to a linear combination of reference spectra for each component (converted to mass absorption scale). An energy-independent (constant) term (a_o) is also usually included to accommodate unexpected backgrounds:

$$OD(j,k) = a_o + \Sigma_i \, a_i * OD\text{-model}_i$$

The vertical scale of the derived component maps in either analytical method is the (density*thickness) product of each component. If the density is known, or can be estimated (in many polymer systems it is within 10% of 1.0) then the component maps provide a true thickness map. [Koprinarov 00].

_____

6. Example 2; Quantitative chemical mapping at sub-micron resolution

The second example illustrates an application of image sequence analysis [Croll00]. *Polymer capsules* and particles with tailored walls, and core-shell structures are attractive for a wide number of applications, including separation science applications, adhesives, coating, chemical delivery, etc. [Li99]. In order to optimise for a particular application, e.g. designing the wall properties for controlled release of a specific chemical, one needs to perform accurate quantitative analysis of the chemical structure of the wall at high spatial resolution. The polyurea capsules are made by dispersing a mixture of aromatic isocyanate and xylene in an aqueous solution of a polyamine. Interfacial polymerisation reactions of both the amine and water with the isocyanate occur at the surface of the dispersed hydrophobic, organic droplets. Competition among amine-isocyanate and water-isocyanate reactions is controlled by differences in kinetics and diffusion rates. This can lead to chemically structured capsule walls. The amine-isocyanate reaction forms an asymmetric (aromatic-aliphatic) urea whereas the water-isocyanate forms a symmetric di-aromatic urea.

We have used quantitative NEXAFS microscopy to visualize the gradient of chemical composition across a capsule wall formed in this manner. **Figure 9** presents component maps derived from image sequences using singular value decomposition and model spectra taken from
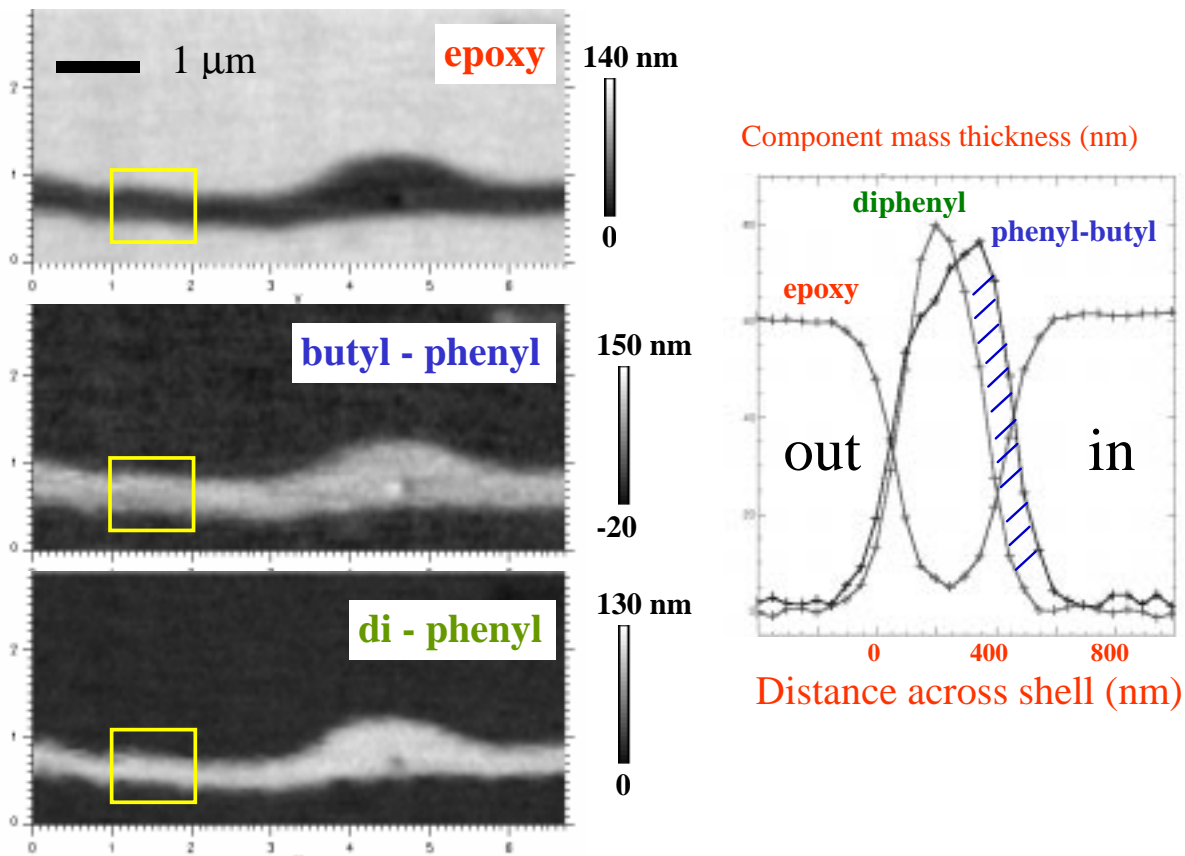
Fig. 9 Quantitative compositional maps for the epoxy, symmetric (di-aromatic) and the asymmetric (aromatic-aliphatic) urea components, derived by SVD analysis of C 1s image sequences of the urea capsule. Profiles of the three components across the capsule wall averaged over the same region (box). These profiles indicate there is an excess of symmetric urea at the outer part of the wall, a balance in the middle of the wall, and a large excess of the asymmetric urea on the inner part of capsule wall.

small molecule analogues. The vertical scale of these maps represents the thickness in nm of that component. The profiles across the capsule wall in the region marked on the maps, show that there is an internal chemical structure to the capsule wall, and that this structure reflects the expected changes arising from the synthetic methodology. In particular, the symmetric di-aromatic urea from the water-isocyanate reaction is a narrower band at the outer region of the wall, whereas the asymmetric urea arising from the amine-isocyanate reaction is thicker and extends all the way to the inner side of the capsule wall. Please note that the total wall thickness is only 500 nm and the differences in chemical composition are observed with better than 100 nm spatial resolution. This precision of chemical quantification at high spatial resolution demonstrates that STXM is a powerful analytical tool which can provide assistance in the development of structured polymeric systems which cannot be provided by any other technique.

Outlook

There are only a few STXM microscopes in the world. The instrumentation was originally developed by Kirz and collaborators (SUNY-Stony Brook) and the Kirz and Jacobsen groups operate three STXM at the X1 undulator beamline at the National Synchrotron Light Source in Brookhaven. At the Advanced Light Source, there is one operating STXM on beamline 7.0. An upgrade of this microscope will be installed in fall 2000. A second STXM beamline dedicated to polymer and soft materials analysis is under construction at the ALS. It will be operational by the end of 2000. A third centre for STXM is the King's College instrument at beamline 5U2 in Daresbury, England. Other STXM instruments are under construction at BESSY II in Berlin, at Daresbury and at the Korean synchrotron.

If you are interested in analytical studies of polymers or other materials using STXM or other X-ray microscopy techniques, please contact

Adam Hitchcock
BIMR
McMaster University
Hamilton, ON L8S 4M1 Canada
Tel: 905 525-9140 ext 24749
E-mail: aph@mcmaster.ca

Acknowledgements

References

[ade 92]   H. Ade, X. Zhang, S. Cameron, C. Costello, J. Kirz, and S. Williams, *Science*, **258**, 972 (1992)

[ade 93]   H. Ade and B. Hsiao, *Science*, **262**, 1427 (1993)

[Ade 95]   H. Ade, A. Smith, S. Cameron, R. Cieslinski, C. Costello, B. Hsiao, G.E. Mitchell, and E.G. Rightor, *Polymer*, **36**, 1843 (1995).

[ade 97]   H. Ade, A.P. Smith, H. Zhang, B. Winn, J. Kirz, E. Rightor and A.P. Hitchcock, *J. Electron Spectrosc.* **84**, 53 (1997).

[ade 98]   H. Ade, in *Experimental Methods in the Physical Sciences*, Vol. 32, pp. 225, J.A.R. Samson and D.L. Ederer Ed., Academic Press, 1998.

[ade 00]   H. Ade and S.G. Urquhart, *Chemical Applications of Synchrotron Radiation* ed. TK Sham, (World Scientific, 2000, in press)

[Croll 00]   L.M. Croll, I. Koprinarov, A.P. Hitchcock, W.H. Li, and H. Stöver, in preparation.

[Egerton 87]   R. E. Egerton, P. A. Crozier, P. Rice, *Ultramicroscopy*, **23**, 305 (1987).

[hitchcock 00-a]   A. P. Hitchcock, I.Koprinarov, T. Tyliszczak, E. G. Rightor, G. E. Mitchell, M. T. Dineen, W. Lidy, R. D. Priester, S. G. Urquhart, A. P. Smith, H. Ade, submitted.

[hitchcock00-b]   A.P. Hitchcock, I. Koprinarov, K. Pecher, and E.M. Kneedler, in preparation

[jacobsen 00]   C. Jacobsen, S. Wirick, G. Flynn, and C. Zimba, *J. Microscopy* **197**, 173 (2000).

[Kirz96]   J. Kirz, C. Jacobsen and M. Howells, Quarterly Review of Biophyisics, **33** , 33 (1995).

[Koprinarov 00]   I. Koprinarov, A.P. Hitchcock, K. Dalnoki-Varess, C. Murray, J. Dutcher, and H. Ade, in preparation.

[Li99]   W.-H. Li and H.D:H Stöver, J. Polym. Sci., Polym. Chem. **37**, 2295 (1999).

[mitchell99]   G.E. Mitchell et al, ALS Compendium of Abstracts, 1999

[press 92]   W.H. Press, et al. *Numerical Recipes in C: The Art of Scientific Computing.* Cambridge: Cambridge University Press, 1992.

[rightor 97]   E.G. Rightor, A.P. Hitchcock, H. Ade, R.D. Leapman, S.G. Urquhart, A.P. Smith, G. Mitchell, D. Fischer, H.J. Shin and T. Warwick, *J. Phys. Chem.* B **101**, 1950 (1997).

[Smith 96]   A. P. Smith and H. Ade, *Appl. Phys. Lett*. **69**, 3833 (1996)

[Stohr 92]   J. Stöhr, *NEXAFS Spectroscopy*, Springer-Verlag, Berlin, 1992.

[strang88]   G. Strang, *Linear Algebra and Its Applications.* San Diego: Harcourt Brace Jovanovich, 1988

[warwick 97]   T. Warwick, H. Padmore, H. Ade, A.P. Hitchcock, E.G. Rightor and B. Tonner, J. Electron Spectrosc. **84**, 85 (1997).

[warwick 98]   T. Warwick, K. Franck, J.B. Kortwight, G. Meigs, M. Moronne, S. Myneni, E. Rotenberg, S. Seal, W.F. Steele, H. Ade, A. Garcia, S. Cerasari, J. Denlinger, S. Hayakawa, A.P. Hitchcock, T. Tyliszczak, E.G. Rightor, H.-J. Shin and B. Tonner, *Rev. Sci. Inst*. **69,** 2964 (1998).